



Communication

Polymorphism in $\text{MnSe}_{1-x}\text{Te}_x$ thin-filmsO.B. Romanova^{a,b,*}, S.S. Aplesnin^{a,c}, M.N. Sitnikov^c, A.M. Kharkov^c, A.N. Masyugin^c, K.I. Yanushkevich^d^a Kirensky Institute of Physics, Federal Research Center KSC SB RAS, 660036, Krasnoyarsk, Russia^b Siberian Federal University, 660041, Krasnoyarsk, Russia^c Siberian State Aerospace University of Science and Technology named after ac. M F Reshetnev Corporation, 660037, Krasnoyarsk, Russia^d Scientific-Practical Materials Research Center NAS of Belarus, 220072, Minsk, Belarus

ARTICLE INFO

Communicated by E.L. Ivchenko

Keywords:

A. Polycrystalline films

C. Structure

D. Polymorphic transition, kinetic properties

ABSTRACT

To establish the polymorphic transition in polycrystalline $\text{MnSe}_{1-x}\text{Te}_x$ ($0.1 \leq X \leq 0.2$) films, their structural, magnetic, kinetic, and optical properties have been investigated in the temperature range of 77–800 K and magnetic fields of up to 12 kOe. Using X-ray diffraction analysis, the coexistence of two crystalline phases in the films has been found. The magnetic moment of the films has been shown to increase with the increasing substitute concentration and decreasing temperature. The impedance maxima and thermopower sign change in the region of the polymorphic and magnetic transitions have been observed. The variation in the structural characteristics has been established using the infrared spectroscopy and thermal expansion coefficient data. The experimental results are explained within a model of domains and domain walls.

1. Introduction

Chalcogenides belonging to the systems with strong electron correlations attract much attention due to the strong interrelation of the magnetic, electric, and lattice subsystems, which manifests itself at the metal–dielectric phase transitions, as well as in the colossal magnetoresistance [1–5]. The best-studied chalcogenide compound is a *p*-MnSe semiconductor characterized by polymorphism [6–8]. A distinguishing feature of manganese monoselenide is the coexistence of two phases: cubic NaCl (about 70%) and hexagonal NiAs (about 30%) below $T < 266$ K [9,10]. The temperature of magnetic phase transition in NiAs coincides with the temperature $T_S = 266$ K of the structural transition; for the cubic modification, $T_N = 135$ K. The MnSe compound exhibits the magnetoresistive effect in the magnetically ordered phase [11]. Manganese monotelluride has a NiAs-type hexagonal structure it is an antiferromagnet with a Neel temperature of $T_N = 310$ K [12–14]. The Neel temperature of antiferromagnetic manganese monotelluride increases under pressure from $T_N = 310$ K to $T_N = 520$ K at $P = 8$ GPa and the gap in the electron excitation spectrum halves. According to the theoretical band-structure calculations, a decrease in the Mn–Te metal–anion bond length induces the crystal structure variation from hexagonal (H) to cubic (ZB) with an energy differences of $dE_{ZB,H} = -0.21$ eV/(bond) per Mn–Te bond with a length of $R_{AF} = 2.70$ Å for the antiferromagnetic ordering and

$dE_{ZB,H} = -0.40$ eV/(bond) per bond with a length of $R_F = 2.71$ Å for the ferromagnetic ordering [15–17]. The lattice constant $a = 0.544$ nm of MnSe with the NaCl structure lies near $2R_F$; therefore, substitution of tellurium for selenium can lead to the formation of MnTe clusters with the ferromagnetic ordering and distorted cubic structure. The quasi-degeneracy is lifted in electric or magnetic fields and under pressure.

Substitution of tellurium ions with the large ionic radius for selenium in the bulk $\text{MnSe}_{1-x}\text{Te}_x$ samples stabilizes the cubic structure at concentrations of up to $X = 0.4$ [18]. According to the neutron diffraction data, the compositions with $X > 0.4$ exhibit the polymorphic properties, i.e., are characterized by the coexistence of two crystalline phases with the different symmetries, cubic (NaCl) and hexagonal (NiAs), over the entire temperature range of 77–300 K [19]. Anion substitution in manganese monoselenide leads to the variation in the exchange coupling sign, formation of an impurity subband near the Fermi level at the low substitute concentrations, magnetic moment variation, and a decrease in the activation energy [18,20]. The magnetic structure rearrangement caused by the competition of the ferro- and antiferromagnetic interactions and splitting of the band of spin-polaron states in the impurity subband can lead to the high magnetic-field sensitivity of the transport properties. In the bulk samples with $X = 0.1$, the negative 100-% magnetoresistance near the Neel temperature was found [18].

At the transition from the bulk samples to thin-film MnSe and MnTe

* Corresponding author. 660036, Krasnoyarsk, Akademgorodok, 50, str. 38, Russia.

E-mail address: rob@iph.krasn.ru (O.B. Romanova).

compounds, the Neel temperature and activation energy decrease manifold [21–23]. The cubic (NaCl) and hexagonal (NiAs) structures are stabilized in the MnSe and MnTe films, respectively [24–26]. It is expected that the polycrystalline thin-film $\text{MnSe}_{1-x}\text{Te}_x$ samples should exhibit new effects and characteristics that distinguish them from the bulk analogs.

The aim of this work was to establish polymorphic transitions in the anion-substituted $\text{MnSe}_{1-x}\text{Te}_x$ thin-film chalcogenide system by complex study of its structural, optical, and kinetic properties.

2. Synthesis, structure and magnetic properties of the films

Thin-films $\text{MnSe}_{1-x}\text{Te}_x$ compounds with a concentrations ($0.1 \leq X \leq 0.2$) were synthesized by thermal evaporation.

X-ray diffraction analysis of the $\text{MnSe}_{1-x}\text{Te}_x$ ($0.1 \leq X \leq 0.2$) thin films was performed on a DRON-3 diffractometer (CuK α radiation) at a temperature of 300 K after their deposition and after the measurements of the magnetic and galvanomagnetic properties. The X-ray diffraction data show that the transition from the bulk samples to nanostructured thin films is accompanied by the crystal symmetry change. In the films with the low substitute concentration ($X = 0.1$), a face-centered cubic (fcc) structure prevails. As the substitute concentration increases to $X = 0.2$, additional peaks corresponding to the hexagonal nickel arsenide structure arise in the X-ray diffraction pattern of the $\text{MnSe}_{1-x}\text{Te}_x$ film system. The intensity of peaks corresponding to the cubic structure decreases with an increase in the tellurium concentration (Fig. 1). The calculated lattice parameters for the films are given in Table 1.

The transition from the bulk samples to thin films leads to the change in the magnetic characteristics of $\text{MnSe}_{1-x}\text{Te}_x$. Fig. 2a and b presents temperature dependences of the magnetic moment for the polycrystalline $\text{MnSe}_{0.9}\text{Te}_{0.1}$ and $\text{MnSe}_{0.8}\text{Te}_{0.2}$ films obtained in a magnetic field of 8.6 kOe. The measurements were performed on the

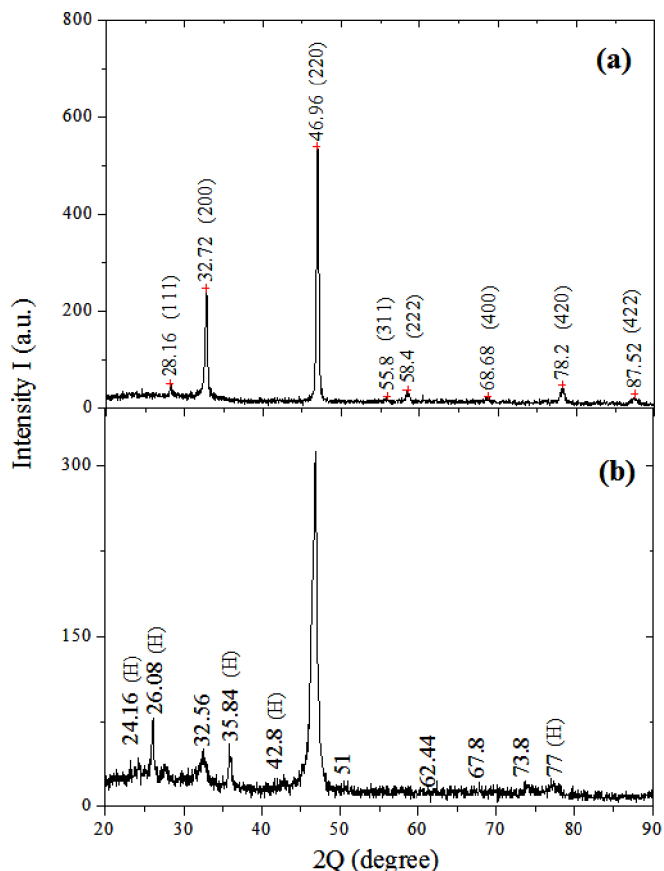


Fig. 1. XRD patterns of the thin-films $\text{MnSe}_{0.9}\text{Te}_{0.1}$ (a) and $\text{MnSe}_{0.8}\text{Te}_{0.2}$ (b).

Table 1
Structural characteristic of thin-film system $\text{MnSe}_{1-x}\text{Te}_x$ samples.

Composition $\text{MnSe}_{1-x}\text{Te}_x$	a, nm	c, nm
X = 0.1 (cubic structure)	0.54736	–
X = 0.2 (cubic structure + hexagonal structure)	0.39283	0.55282

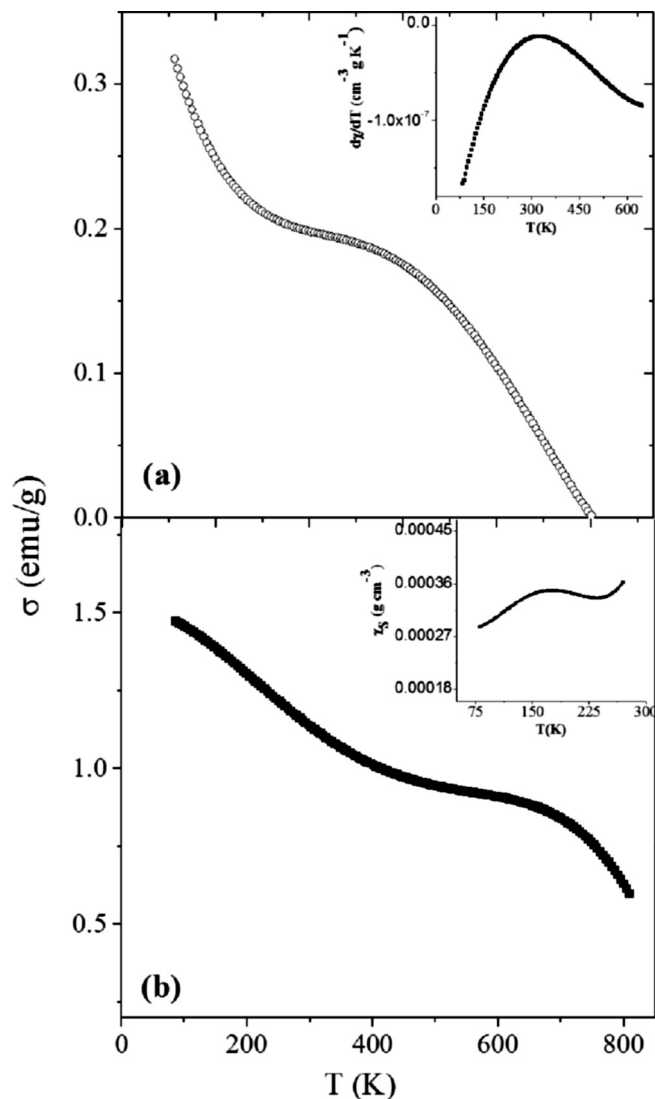


Fig. 2. The temperature dependence of the magnetization of the polycrystalline films $\text{MnSe}_{0.9}\text{Te}_{0.1}$ (a) and $\text{MnSe}_{0.8}\text{Te}_{0.2}$ (b) measured in a magnetic field of 8.6 kOe. Inset: a - the derivate of the susceptibility for $\text{MnSe}_{0.9}\text{Te}_{0.1}$; b - temperature dependence of the susceptibility of the composite system MnSe - MnTe.

samples placed in evacuated quartz ampoules. Using the magnetic susceptibility derivative $d\chi/dT$ (inset in Fig. 2a), we determined the magnetic transition temperature $T_N = 322$ K for the samples with $X = 0.1$ and $T_N = 300$ K for the samples with $X = 0.2$, which is almost twice as high as the temperature of magnetic transition determined for the bulk samples with the analogous compositions [18]. The temperature dependences of magnetization of the bulk samples have maxima at $T_N = 132$ K ($X = 0.1$) and 130 K ($X = 0.2$). This is indicative of the increased contribution of the MnTe system due to the formation of hexagonal NiAs nanoareas containing an odd number of ferromagnetically coupled planes. If the magnetic moment of a film is determined by a sum of magnetic moments of manganese ions with the cubic and

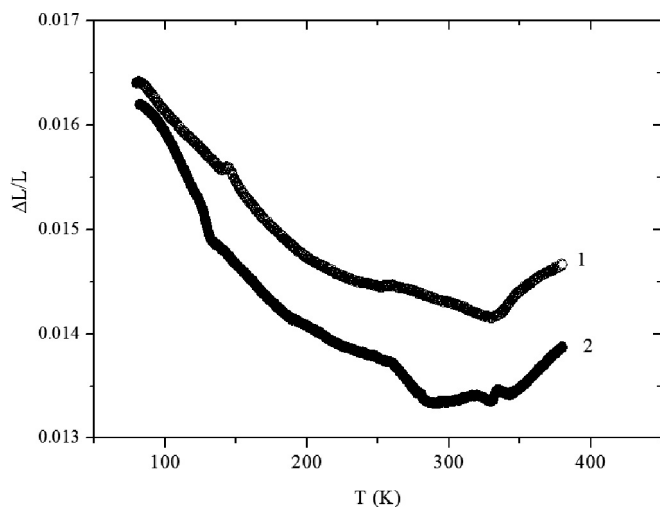


Fig. 3. The temperature dependence of the relative change in the film length for $\text{MnSe}_{0.9}\text{Te}_{0.1}$ (1) and $\text{MnSe}_{0.8}\text{Te}_{0.2}$.

hexagonal structures, the susceptibility of the system monotonically increases with temperature (inset in Fig. 2b), which contradicts the experimental data. This fact points out the interaction of magnetic structures. The growth of the density of intergrain boundaries during the polymorphic transition leads to the additional contribution to the film magnetization. The occurrence of the polymorphic transition is confirmed by the change in linear sizes of the film.

The lattice strain caused by the structural transitions can be determined by measuring the electrical resistance of strain gauges located in the film and quartz: $(R^f(T) - R^q(T))/R^q(T) = (L^f(T) - L^q(T))/L^q(T) = \Delta L$. The linear expansion coefficient of quartz is $0.8 \cdot 10^{-6} \text{ K}^{-1}$. Fig. 3 illustrates the relative change in the film length with temperature for the polycrystalline $\text{MnSe}_{1-x}\text{Te}_x$ ($X = 0.1$ and 0.2) films. It can be seen that as the substitute concentration grows, the relative change in the film length increases. The $\Delta L/L(T)$ dependence contains anomalies at temperatures of $\sim 330 \text{ K}$ and $130\text{--}140 \text{ K}$, which correspond to the transitions to the magnetically ordered state with the NiAs and cubic structure. These transitions are induced by the magnetoelastic interaction. In the $\Delta L/L(T)$ dependence, we found a step anomaly in the region of the polymorphic transition at $T_p = 260 \text{ K}$. At $X = 0.2$, this anomaly is even more pronounced (the step is sharper). The occurrence of two phases in the sample facilitates its polymorphism.

3. Kinetic and optical properties of the films; discussion

The polymorphic transition in the polycrystalline films result in the variation in the magnetic properties, as well as to the electronic structure rearrangement. For the polycrystalline $\text{MnSe}_{1-x}\text{Te}_x$ ($X = 0.1$ and 0.2) films, we measured the active (real part) and reactive (imaginary part) resistances and the impedance $Z = Z' + iZ''$ (Z' and Z'' are the real and imaginary parts of the impedance, respectively) in the frequency band of $\omega = 1\text{--}1000 \text{ kHz}$ at temperatures of $80\text{--}400 \text{ K}$ with the use of an AM-3028 component analyzer. The temperature dependence of the impedance for the films with $X = 0.1$ and 0.2 (Fig. 4a and b) contains two broad maxima, one corresponding to the transition to the magnetically ordered state and the other, to the polymorphic transition. As the tellurium concentration increases, the density of intergrain boundaries grows, which leads to the impedance increasing. The main contribution to the impedance is made by the capacitance, which is confirmed by the linear frequency dependence of its imaginary part at constant temperature. The imaginary part of the impedance measured in the frequency band of $1\text{--}1000 \text{ kHz}$ is described well by the function $\text{Im}Z = 1/\omega C$ with the capacitance growing upon heating. The linear $\text{Im}Z(\omega)$ dependence confirms the existence of electrically

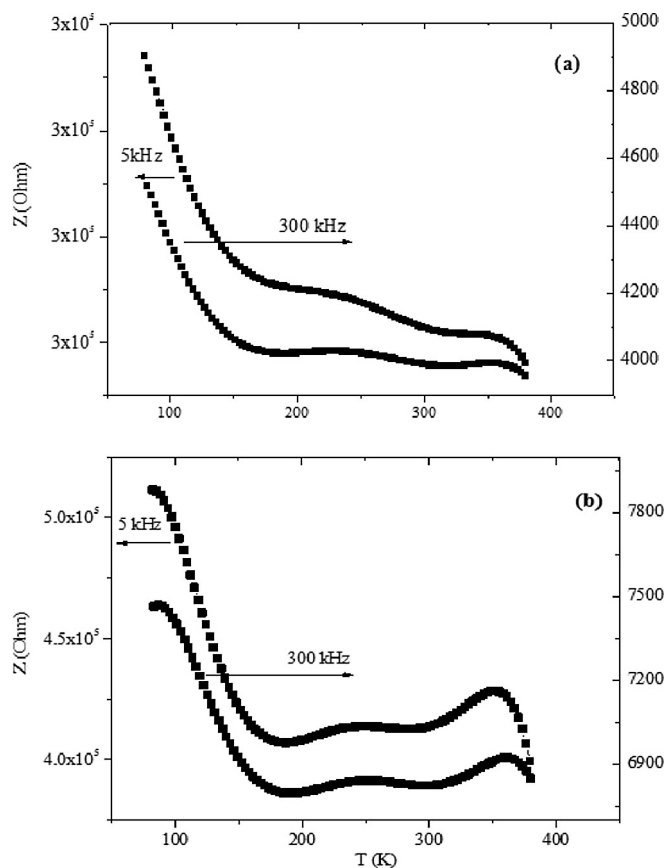


Fig. 4. The temperature dependences of the impedance of polycrystalline films $\text{MnSe}_{0.9}\text{Te}_{0.1}$ (a) and $\text{MnSe}_{0.8}\text{Te}_{0.2}$ (b), measured at frequencies 5 kHz (1) and 300 kHz (2).

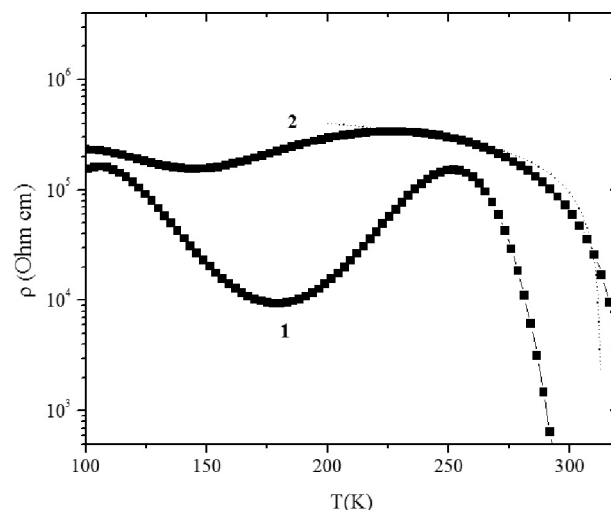


Fig. 5. The temperature dependence of the electrical resistivity for films $\text{MnSe}_{0.9}\text{Te}_{0.1}$ (1) and $\text{MnSe}_{0.8}\text{Te}_{0.2}$ (2). The temperature dependence of the resistance is described by a power function (1) (The dotted line).

nonuniform states in the film.

The temperature dependence of the impedance differs from the behavior of dc resistance (Fig. 5). The temperature dependence of resistance for the composition with $X = 0.1$ reveals the maximum caused by the polymorphic transition, which smooths with increasing substitute concentration. Carrier transport can be realised via electron hoppings between domain walls or due to diffusion of walls. These are activation processes, in which the electron mobility is determined as

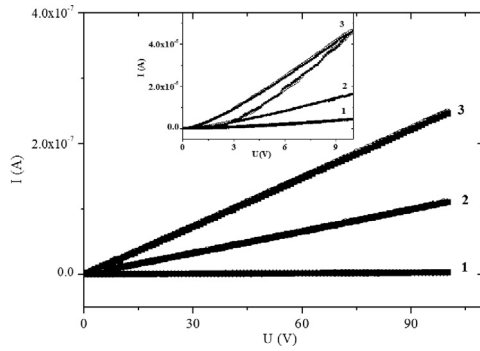


Fig. 6. The current-voltage characteristics measured in a zero magnetic field (empty circles) and field 12 kOe (black circles). $\text{MnSe}_{0.9}\text{Te}_{0.1}$ at $T = 80$ K(1), 180 K(2) and 220 K(3). Inset: $\text{MnSe}_{0.8}\text{Te}_{0.2}$ at $T = 80$ K(1), 180 K(2) and 280 K(3).

$\mu = \mu_0 \exp(-E_a/k_0T)$, where $\mu_0 = ea^2v/k_0T$, v is the hopping frequency equal to the phonon frequency ($\sim 10^{13}$ Hz), and a is the distance between domain walls [27]. The diffusion of walls can result from the interaction with acoustic spin waves. The wall flow is proportional to the diffusivity $j \sim D \sim v\lambda$, where v is the spin wave velocity and λ is the free path proportional to the spin correlation radius $\lambda \sim \xi = B/(1 - T/T_N)$. The more the number of spins deflected from the antiferromagnetic ordering, the smaller the energy loss of wall motion. The diffusion of domain walls in the antiferromagnetic matrix increases with temperature as $D \sim 1/(1 - T/T_N)$. The functional temperature dependence of the conductivity can be written in the form

$$\sigma = A/T \exp(-E_a/kT) + B/(1 - T/T_N) \quad (1)$$

where A and B are the fitting parameters. At $X = 0.2$, function (1) describes the experimental results for $A = 1 \cdot 10^{-3}$, $B = 0.4 \cdot 10^{-6}$, and $E_a = 0.021$ eV. Above 200 K, the diffusion contribution prevails and below 200 K, carrier tunneling occurs mainly via hoppings.

The existence of domain walls above the temperature of the polymorphic transition is confirmed by the I - V characteristics measured at constant temperatures in zero magnetic field and in a field of 12 kOe. Fig. 6 presents the I - V characteristics for the polycrystalline $\text{MnSe}_{1-x}\text{Te}_x$ ($X = 0.1$ and 0.2) films. For the samples with the low substitute concentration ($X = 0.1$), the I - V characteristics are linear and independent of applied field over the entire temperature range. At the higher concentration, the I - V characteristics have a hysteresis above the temperature of the polymorphic transition; the hysteresis width decreases in magnetic field and, under a voltage of above 6 V, the hysteresis width changes by (10–20) %. As the magnetic field increases, the density of domain walls decreases together with their mobility.

The data on thermopower coefficient allow us to determine the carrier sign in the absence of dragging electrons with phonons or magnons. Fig. 7 shows temperature dependences of the thermopower coefficient for the composition with $X = 0.2$. As the temperature increases, the sign change from positive ($\alpha > 0$) to negative ($\alpha < 0$) is observed at coming to the polymorphic transition, which is indicative of the change in the majority carrier type from hole to electron or dragging electrons with magnons (domain walls). Upon approaching the Neel temperature, domain walls vanish and thermopower is caused by diffusion of holes, which changes the thermopower sign.

The presence of crystal lattice defects was established by infrared (IR) spectroscopy. The optical properties of the polycrystalline $\text{MnSe}_{1-x}\text{Te}_x$ ($X = 0.1$ and 0.2) films were studied on a FSM 2202 IR Fourier spectrometer. The measurements were performed in an optical cryostat in the temperature range of 77–500 K. The IR spectra shown in Fig. 8 have two peaks at frequencies of $\omega \sim 3500$ cm^{-1} (peak A) and ~ 4000 cm^{-1} (peak B). We attribute these peaks to the impurity state in the lattice, the energy of which is determined by the crystal symmetry. At the heating, the intensity of peak A (corresponds to the cubic phase

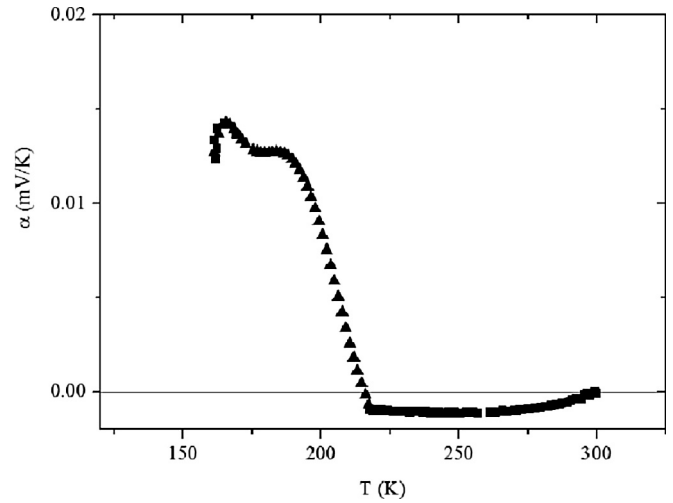


Fig. 7. The temperature dependence of the thermopower for thin-films chalcogenide compound $\text{MnSe}_{0.8}\text{Te}_{0.2}$.

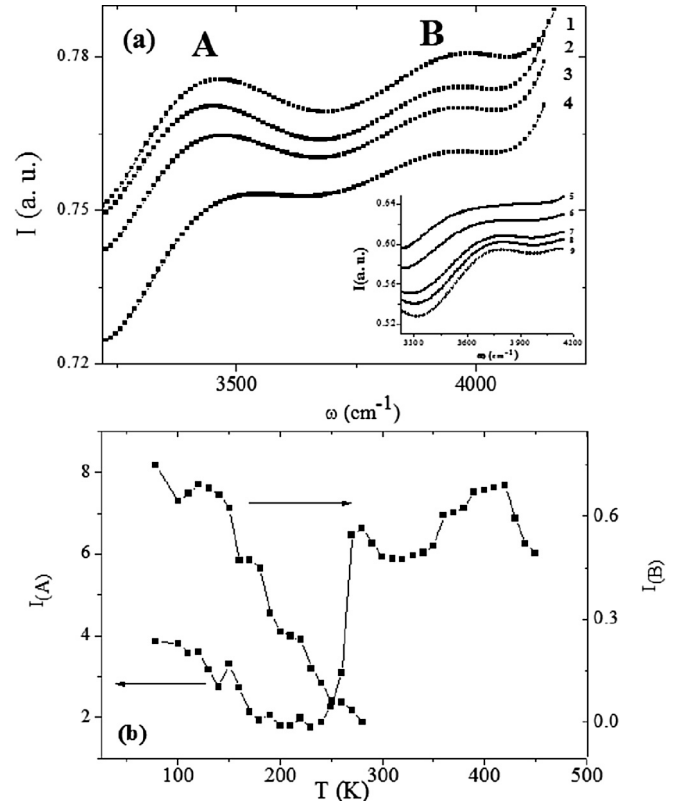


Fig. 8. a - spectra of optical absorption for a polycrystalline film $\text{MnSe}_{0.9}\text{Te}_{0.1}$ measured at different temperatures 1–100 K, 2–130 K, 3–150 K, 4–180 K. Inset: the temperature range 5–300 K, 6–340 K, 7–400 K, 8–430 K, 9–460 K. A and B - two peaks, shown on absorption spectra. The peak A corresponds to the cubic phase, and the peak is B-hexagonal. b- temperature dependence of the absorption intensity (the peaks A and B).

NaCl) increases abruptly and peak B (hexagonal phase NiAs) vanishes in the region of the polymorphic transition (Fig. 8b). The temperature of the latter determined from the optical absorption spectra is consistent with the temperatures of anomalies in the dependences of the relative change in the sample linear sizes and on the dc and ac resistances.

4. Conclusion

Thus, it was established that the transition from the bulk $\text{MnSe}_{1-x}\text{Te}_x$ solid solution samples to thin films leads to the occurrence of polymorphism. The intensity of peaks corresponding to the cubic structure decreases with the increasing tellurium concentration and additional peaks corresponding to the nickel arsenide (NiAs) hexagonal structure arise. Temperature behavior of the susceptibility of the films is qualitatively different from that of the composite system consisting of manganese telluride and selenide. The linear expansion coefficient of the films has anomalies in the regions of magnetic transitions with the NiAs and cubic structure and in the region of the polymorphic transition at $T_p = 260$ K, which is especially pronounced in the samples with $X = 0.2$. The existence of domains and domain walls was confirmed by impedance spectroscopy and I - V hysteresis, which weakens in a magnetic field and originates from a decrease in the density of domain walls in a magnetic field. The change in the sign of the thermopower coefficient with temperature was explained using a model of drag of carriers with domain walls, which vanish near the Neel temperature. Splitting of the IR absorption spectra and maximum electric resistance were found in the region of polymorphic transition. In this region, the correlation of the structural, electrical, kinetic, and optical properties was observed.

Acknowledgements

This study was supported by the Russian Foundation for Basic Research, project no. 18-52-00009 bel_a, № 18-32-00079 mol_a, № 18-42-240001 r_a; the state order № 3.5743.2017/6.7.

References

- [1] V.N. Antonov, L.V. Bekenov, A.N. Yaresko, *Adv. Condens. Matter Phys.* 2011 (2011) 107.
- [2] J.M. Pizarro, M.J. Calderon, J. Liu, M.C. Muñoz, E. Bascones, *Phys. Rev. B* 95 (2017) 075115–075118.
- [3] Yuqiao Guo, Jun Dai, Jiyin Zhao, Changzheng Wu, Diandi Li, Lidong Zhang, Wei Ning, Mingliang Tian, Xiao Cheng Zeng and Yi Xie, *Phys. Rev. Lett.* 113 (2014) 157202–157205.
- [4] S. Borghardt, Jhin-Sian Tu, F. Winkler, J. Schudert, W. Zander, K. Leosson, B.E. Kardynał, *Phys. Rev. Mater.* 1 (2017) 054001–054016.
- [5] M. Safari, Z. Izadi, J. Jalilian, I. Ahmad, S. Jalali-Asadabadi, *Phys. Lett. A* 381 (2017) 663–670.
- [6] M. Bouroushian, *Electrochemistry of Metal Chalcogenides*, Springer-Verlag, Berlin, 2010.
- [7] S.J. Youn, B.I. Min, A.J. Freeman, *Phys. Status Solidi (b)* 241 (2004) 1411–1414.
- [8] M.R. Gao, Y.F. Xu, J. Jiang, S.H. Yu, *Chem. Soc. Rev.* 42 (2013) 2986–3017.
- [9] D. Wolverson, *Phys. Status Solidi (b)* 253 (2016) 1461–1464.
- [10] J.B.C. Efreem D'Sa, P.A. Bhobe, K.R. Priolkar, A. Das, P.S. Rio Krishna, P.R. Sarode, R.B. Prabhu, *Pramana - J. Phys.* 63 (2004) 227–232.
- [11] S.S. Aplesnin, L.I. Ryabinkina, O.B. Romanova, D.A. Balaev, O.F. Demidenko, K.I. Yanushkevich, N.S. Miroshnichenko, *Phys. Solid State* 49 (2007) 1984–1989.
- [12] N.G. Szwacki, E. Przeździecka, E. Dynowska, P. Bogusławski, J. Kossut, *Acta Phys. Pol. A* 106 (2004) 233–238.
- [13] C. Reig, V. Muñoz, C. Gomez, Ch. Ferrer, A. Segura, *J. Cryst. Growth* 223 (2001) 349–356.
- [14] Ch. Ferrer-Roca, A. Segura, C. Reig, V. Muñoz, *Phys. Rev. B* 61 (2000) 13679–13686.
- [15] Bongseo Kim, Inhye Kim, Bok-ki Min, Minwook Oh, Sudong Park, Heewoong Lee, *Electron. Mater. Lett.* 9 (2013) 477–480.
- [16] R.J. Iwanowski, M.H. Heinonen, B. Witkowska, *J. Alloy. Comp.* 491 (2010) 13–17.
- [17] Hitoshi Sato, Takahiro Mihara, Akihito Furuta, Masamochi Tamura, Kojiro Mimura, Naohisa Happpo, Masaki Taniguchi, *Phys. Rev. B* 56 (1997) 7222–15.
- [18] S.S. Aplesnin, O.B. Romanova, K.I. Yanushkevich, *Phys. Status Solidi b* 252 (2015) 1792–1798.
- [19] Kapil E. Ingle1, J.B.C. EfreemD'Sa, A. Das, K.R. Priolkar, *J. Magn. Magn. Magn.* 347 (2013) 68–71.
- [20] S.S. Aplesnin, O.B. Romanova, V.V. Korolev, M.N. Sitnikov, K.I. Yanushkevich, *J. Appl. Phys.* 121 (2017) 075701-7.
- [21] M.A. Angadi, V. Thanigaimani, *Mater. Sci. Eng., B* 21 (1993) L1–L4.
- [22] G.R. Wu, K. Nagatomo, M. Sasaki, F. Nagasaki, H. Sato, M. Taniguchi, W.X. Gao, *Solid State Commun.* 118 (2001) 425–429.
- [23] D. Kriegner, K. Výborný, K. Olejník, H. Reichlová, V. Novák, X. Marti, J. Gaquez, V. Saidl, P. Němec, V.V. Volobuev, G. Springholz, V. Holý, T. Jungwirth, *Nat. Commun.* 7 (2016) 11623–11629.
- [24] T. Mahalingam, S. Thanikaikarasan, V. Dhanasekaran, A. Kathalingam, S. Velumani, Jin-Koo Rhee, *Mater. Sci. Eng., B* 174 (2010) 257–262.
- [25] W. Szuszkiewicz, B. Hennion, B. Witkowska, E. Łusakowska, A. Mycielski, *Phys. Status Solidi (c)* 2 (2005) 1141–1146.
- [26] L. Yang, Z. Wang, D. Li, Z. Zhang, *Vacuum* 140 (2017) 165–171.
- [27] M.Yu. Kagan, K.I. Kugel, *UFN* 171 (2001) 577–596.